Pharm Res (2012) 29:3325–3334
DOI 10.1007/s11095-012-0824-3

RESEARCH PAPER

Penetration of Fluorescein Across the Rabbit Cornea from the Endothelial Surface

Chhavi Gupta • Anuj Chauhan • Sangly P. Srinivas

Received: 12 October 2011 / Accepted: 2 July 2012 / Published online: 20 July 2012

ABSTRACT

Purpose To model the kinetics of penetration of fluorescein across the cornea from the endothelial surface.

Methods Rabbit corneas mounted *in vitro* were exposed to fluorescein at their endothelial surface. Trans-corneal fluorescence were acquired periodically for 6 h using a custom-built confocal microfluorometer. The profiles were then employed to fit a kinetic model for calculation of permeability and diffusion coefficients across the cellular layers and stroma, respectively.

Results At the endothelium-stroma and stroma-epithelium interfaces, the fluorescence profile exhibited sudden jumps. In each case, the fluorescence was higher at the stroma, indicating reduced partitioning of the dye into the lipid-rich cellular layers. The stroma did not swell significantly until 180 min of perfusion. The fluorescence profiles reached a pseudo-steady state at ~6 h. A transport model, which included convective and diffusive fluxes into the stroma, showed a good fit to the trans-corneal profiles at different time points. The estimated permeability coefficients for the cellular layers were close to the values reported previously, but the diffusion coefficient of fluorescein in the stroma was found to be smaller than the values obtained previously using Ussing chambers.

Conclusions The penetration of fluorescein could be modeled accurately by a combination of diffusion and convection.

C. Gupta • A. Chauhan
Department of Chemical Engineering, University of Florida
Gainesville, Florida, USA

S. P. Srinivas (✉)
School of Optometry, Indiana University
800 East Atwater Avenue
Bloomington, Indiana 47405, USA
e-mail: srinivas@indiana.edu

KEY WORDS cornea · diffusion · fluorescein · hydrophilicity · pharmacokinetics

INTRODUCTION

Drug administration to the eye is most frequently accomplished by the topical route. In this approach, the drugs, instilled as drops, on the ocular surface have a brief residence time (half-life ~4 min), during which they access the anterior chamber (a/c) mainly by penetration across the cornea (1,2). The cornea is a tri-laminate structure consisting of epithelium, stroma, and endothelium, and resembles, from a pharmacokinetic point of view, an oil:water:oil matrix. In the human cornea, the epithelium, which forms the anterior surface of the cornea, is ~50 μm thick and is stratified into 5–7 layers. The superficial epithelial layers, known to contribute significantly to the trans-epithelial electrical resistance (3), exhibit multi-stranded tight junctions and therefore form a significant barrier to the penetration of topical drugs. While lipophilic molecules readily penetrate the epithelium by dissolving in the lipid bilayers of the plasma membrane (4), hydrophilic molecules are restricted by the tight junctions as they have to penetrate through the paracellular route. The stroma, the connective tissue component of the cornea, contains ~80% water and hence is hydrophilic. Therefore, stroma offers resistance to transport of hydrophobic molecules but the net transport through cornea increases with hydrophobicity because of the increased transport through the epithelium, which frequently represents the rate limiting step (4). The endothelium, which forms the posterior surface of the cornea, is leaky, and accordingly, does not offer much resistance to the paracellular movement of solutes (5,6).

Drug transport across the cornea has been frequently investigated by mounting the tissue in an Ussing chamber

(7–13). The flux across the tissue is then measured by setting up a concentration differential between the chambers facing the epithelium and endothelium. While such measurements are useful for an understanding of drug penetration, a mechanistic examination of the transport is limited. This is because the trans-corneal concentration profiles of drugs cannot be easily measured, and accordingly, the entire cornea is treated as a homogenous (i.e., well-mixed) compartment. The calculations of permeability of the drugs from such lumped models can be made only after the concentrations in the various layers reach a pseudo-steady state. This takes much longer than the residence time of topical drops (1,2). Thus, it is not valid to utilize the permeability measurements obtained from Ussing chamber experiments. Moreover, the resistance offered by each layer cannot be assessed; hence, whether drug transport is achieved by the transcellular or paracellular route cannot be assessed.

Some of the above drawbacks can be addressed by making use of fluorescent compounds as drug analogs (4). Given the transparency of the cornea, it is possible to determine the depth-resolved trans-corneal fluorescence profile to assess the penetration kinetics of fluorescent substances (14,15). The kinetic parameters, thus obtained, can be correlated to physicochemical properties of the compounds. In a previous publication (4), we employed a custom-built confocal scanning fluorescence microscope to determine the depth-resolved trans-corneal penetration of Rhodamine B (RhB) to exemplify the transport mechanisms typical of a lipophilic molecule. The time- and depth-resolved fluorescence profiles of RhB were then fitted to a multi-scale transport model (4). The RhB profiles and our model showed that transport of hydrophobic molecules across the cellular layers occurs *via* the lipid bilayers with a characteristic slow intracellular accumulation. Transport of RhB from the lipid bilayers to the hydrophobic domains inside the cells was found to be responsible for the slow accumulation, which creates a depot effect for the delivery of drugs to the a/c (4).

In this study, we have adopted a similar approach to explore the transport of a relatively hydrophilic molecule fluorescein across the cornea. Hydrophilic molecules encounter significant resistance to transport across epithelium and endothelium due to the high lipid content of the cellular layers. The resistance of the endothelium is likely substantially smaller than that of epithelium because of the smaller thickness. In most practical situations drugs are delivered into the tears and the drugs diffuse from the epithelium towards the a/c. Due to the large resistance offered by the cornea to diffusion of the hydrophilic molecules, the transport of fluorescein from tears to a/c will be rate limited by epithelium. Thus the concentration profile in the stroma and the endothelium will likely be at a pseudo-steady state which will prevent accurate determination of the transport parameters for these two layers. Furthermore due to the slow diffusion across the epithelium, an experiment in which fluorescein is instilled on the tear side will be required to be performed for a longer period of time which is not feasible due to deterioration in the integrity of cornea with time. It is thus preferable to study diffusion of fluorescein from the a/c towards the epithelium, as described below in the methods section. The time and spatially resolved fluorescence data in the stroma is modeled through a convection-diffusion model, while endothelium and epithelium are modeled as lumped systems with uniform spatial concentration. The convective transport is included in the stroma from the a/c towards the epithelium to account for stromal swelling as noticed in the data. The fluorescence data is fitted to the mathematical model to obtain all the relevant transport and the partition coefficients in the various layers of the cornea. Finally the reliability of the parameters is assessed by parametric sensitivity analysis.

The mechanisms of fluorescein transport explored here were found to be significantly different from those of RhB. Hence, this study along with our previous report (4), is very valuable in understanding the effects of relative hydrophobicity of solutes on transport across the cornea.

MATERIALS AND METHODS

Sodium fluorescein and reagents for Ringers were obtained from Sigma Chemical Company (St. Louis, MO). Eyes were obtained from freshly euthanized albino (New Zealand White) rabbits of both sexes. All procedures for animal handling were followed in accordance with the guidelines set by the Association for Research in Vision and Ophthalmology (ARVO) and were approved by the Laboratory Animal Care Committee in the laboratory of the (late) Prof. DM Maurice, Ophthalmology at Stanford University, CA.

A schematic of the experimental setup used in this study is shown in Fig. 1 and was similar to earlier reports (14,15). The corneas were isolated, mounted, and maintained at 34° C and perfused with HCO_3^- Ringers (containing reduced glutathione, glucose, adenosine, 20 mM HEPES, and 25 mM $NaHCO_3$) both at the anterior and posterior surfaces. The corneal thickness was allowed to stabilize for ~30 min, and then the endothelial surface was exposed to fluorescein dissolved in the Ringers solution (10 μg/mL) as a step change. The trans-corneal profiles of fluorescein were obtained using a custom-built confocal scanning microfluorometer, which has been described previously (14,15). Depth scanning was performed through a stepper motor coupled to the fine focus knob of the microscope. The depth resolution for trans-corneal fluorescence scan was ~8 μm at a sensitivity of 10^{-6} g/mL of fluorescein (SNR > 20) using a

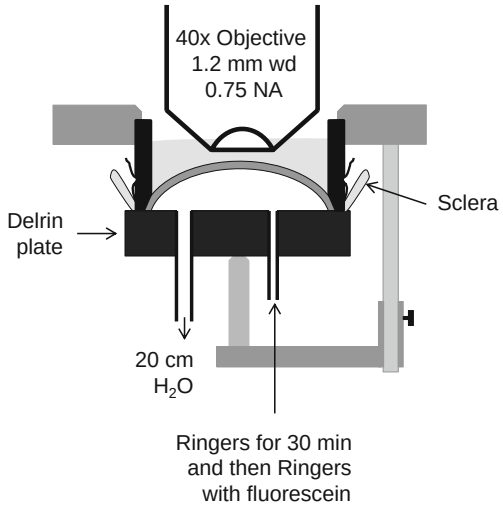

Fig. 1 Schematic representation of the experimental design for *in vitro* mounting of cornea in a diffusion cell. The perfusion medium in the a/c is circulated through a pump. The outflow from the a/c was passed through the larger bore tubing to a height of 20 cm in order to keep the cornea inflated under its normal pressure. The tube diameter for flow in and out of the a/c is sufficiently large to ensure negligible pressure drop across the tubes, ensuring that pressure in a/c is independent of the flow rate of the perfusion medium.

40x water immersion objective of 0.75 NA (Zeiss Inc; working distance=1.5 mm). The excitation and emission wavelengths were 485±10 nm and 530±10 nm, respectively. Scanning was performed at 600 µm/min over 1200 µm depth. Eight experiments were performed identical to the protocol used in this study, out of which six eyes could be maintained healthy for >4 h. The data set from one such experiment (i.e., obtained with one rabbit cornea) has been used for modeling purposes. Although there were variations in the total duration of the experiment between corneas, there were no remarkable variations regarding penetration of fluorescein.

RESULTS

Fluorescence Profiles After Exposure of the Endothelial Surface to Fluorescein

The trans-corneal fluorescence profiles are plotted in Fig. 2 at different time points after introduction of fluorescein into the chamber bathing the endothelial surface (referred to as anterior chamber or a/c). The fluorescence in the a/c is constant as the fluorescein-containing medium is continuously perfused. The region of decreased fluorescence adjacent to the a/c corresponds to the endothelium. The fluorescence increases in the stroma compared to the endothelium due to the hydrophilic nature of fluorescein and the stroma. The fluorescence in stroma decreases along the direction of its diffusion towards the tear side. Finally the fluorescence in the epithelium is negligible for a long time due to the small permeability of the layer to the hydrophilic fluorescein. The fluorescence in stroma is both time- and space-dependent but the space-dependence of fluorescence in the epithelium and endothelium is not resolvable.

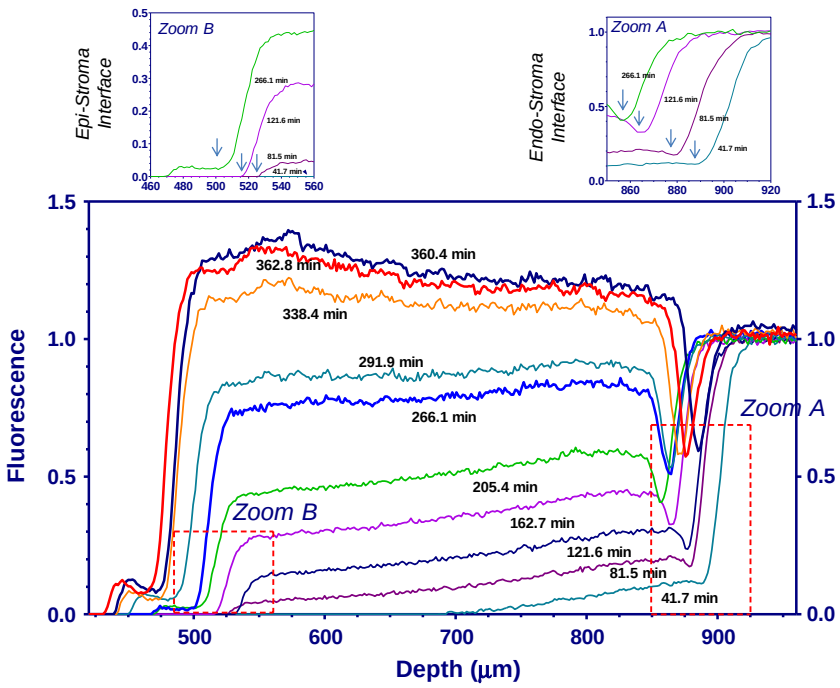

Fig. 2 Transient concentration profiles of fluorescein across the rabbit cornea, when the endothelium side was exposed to a fixed concentration of the dye; Y-axis represents fluorescence in arbitrary units (AU). The fluorescence scans were obtained with a custom-built scanning microfluorometer (see Methods) with a depth resolution of ~8 μm using a 40x objective (Zeiss, Inc. 0.75 NA; water immersion).

Swelling of the Cornea

The thickness of the various layers of the cornea can be determined by utilizing the jumps in fluorescence profiles at the interface of stroma with the cellular layers as a result of partitioning fluorescein as noted above (Fig. 2). Such fluorescence discontinuities are, however, convolved with the instrument response function (IRF). Thus, the location of each of the interfaces can be detected by calculating the slope of the concentration profiles and determining the local maxima of the slope. After the interfaces are located, the thickness of each layer can be determined as the distance between the relevant interfaces. The thicknesses of the epithelium, the stroma, and the endothelium are denoted by L_E, L_S, and L_{En}, respectively. The thickness of the stroma and that of the epithelium are plotted as a function of time in Fig. 3. It is evident from Fig. 3 that the thickness of the stroma is relatively unchanged in the first 200 min but shows an increase at a relatively constant rate of 0.5 μm/min. The thickness of the epithelium is also constant for the first 200 min, but subsequently shows rapid swelling (at 10 μm/h).

DISCUSSION

Fluorescence Profiles After Exposure of the Endothelial Surface to Fluorescein

The fluorescence profiles in Fig. 2 demonstrate that fluorescein partitions into various layers of the cornea and diffuses from the endothelium towards the epithelium following step change in the a/c fluorescein concentration. At 81 min and beyond, fluorescence in the stroma is higher compared to that at the epithelial and endothelial layers (Fig. 2). This is consistent with the hydrophilic nature of fluorescein and the high water content of the stroma. Next, we note that the fluorescence in the endothelium (indicated by arrows in Fig. 2; right insert), represented by the fluorescence minima at the troughs (indicated by arrows) noted between the perfusion chamber and stroma, increases with time, as does the fluorescence in the stroma. This observation suggests that fluorescein is diffusing across the lipid bilayers of the endothelium and accumulating in its cytoplasm. In contrast with the changes in the fluorescence of the endothelium, its increase in the epithelium is not apparent up until 205 min. This is apparent by the fact that the penetration depth of fluorescein into the stroma (i.e., concentration boundary layer thickness) is ~175 μm at 42 min. However, the penetration extends to the stroma-epithelium interface, which is 350 μm away from the endothelium, in <81 min.

If fluorescein were to diffuse only through the paracellular route, then the concentration of fluorescein in the endothelium would be small and independent of time. In fact, the ratio of fluorescence at the stroma-endothelium interface (indicated by filled circles) to that of fluorescence from the endothelium (cytoplasm; indicated by arrows) is relatively constant and concentration in endothelium increases with time. This is shown in Fig. 4 and indicates that the concentrations in the endothelium and in the stroma at the stroma-endothelium boundary are in equilibrium. These observations together suggest that the dominant mechanism for the transport of fluorescein across the endothelium is the transcellular route through the lipid bilayers of the endothelium.

Regarding the penetration depth of fluorescein into the stroma, we recall that the thickness of a purely diffusive boundary layer changes as the square root of time. Therefore, the time taken for the boundary layer noted in Fig. 2 to reach a depth of 350 μm should be 4x the time that it took to reach a depth of 175 μm. Since it took 42 min for concentration boundary layer to reach 175 μm (as noted above), it should take ~168 min to reach full thickness of stroma (i.e., 350 μm). However, as shown in Fig. 2 it takes less than 81 min for boundary layer to reach full thickness of

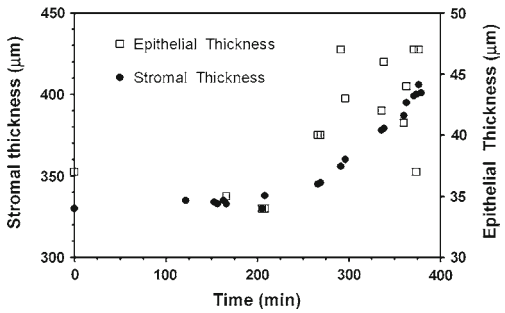

Fig. 3 Transient swelling of corneal layers the stroma and the epithelium. The location of each of the interfaces was specified by local maxima of the slope of the fluorescence profiles. The slope is theoretically infinite due to differences in partitioning of the dye in different corneal layers, but the profiles are smoothed due to the instrument response function.

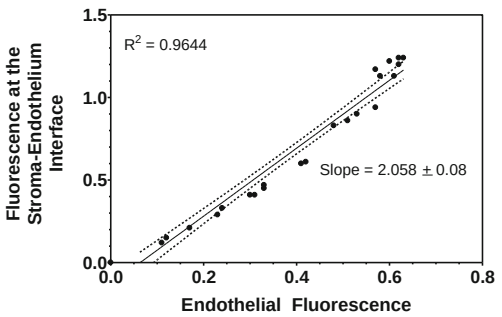

Fig. 4 Relationship between the concentration of fluorescein at the stroma-endothelium interface and the concentration in the endothelium (cytoplasm in the endothelium) with time as the parameter. Both axes represent fluorescence in arbitrary units (AU). The plot is a straight line showing that the ratio of the concentrations is relatively independent of time.

stroma which is much less than 4x the time for the boundary layer to traverse half of the stroma. This observation suggests that fluorescein transport in the stroma must be occurring as a combination of diffusion and convection.

Modeling the Transport of Fluorescein Across the Cornea

Figure 5 illustrates the concentration profile of fluorescein as it is transported from the a/c toward the tear-cornea interface. The barriers for the transport include endothelium, stroma, and epithelium, with the transport mechanisms being different in each layer due to differences in their composition and structure.

The corneal swelling during the experiment, as noted above, complicates the transport model since it implies moving boundaries. Since mechanisms of swelling are not the focus of this paper, we have utilized the data for the first 180 min to model fluorescein transport across stroma and the endothelium. However, during this period, the fluorescence in the epithelium is negligible so that data beyond 180 min is employed to predict epithelial concentrations from the model.

Transport in the Stroma

We approximate the fluorescein transport in the stroma by a combination of diffusion and convection. The latter phenomenon, as noted above, is invoked in the model to account for the apparent fluid movement from the endothelium toward the epithelium. The corneal stroma is composed of about 260 lamellae of collagen fibrils bound with glycosaminoglycans (GAGs). The solute molecules could bind to collagen and GAGs. However, the binding-unbinding events occur on a faster time scale compared to that of diffusion; thus, we assume that the bound and unbound forms are in equilibrium so that we can write only the mass balance for the total solute amount. Therefore, the governing equation for fluorescein transport in the stroma can be written as:

$$D\frac{\partial^2 \mathrm{C}_2}{\partial \mathrm{x}^2} - \mathrm{v}\frac{\partial \mathrm{C}_2}{\partial \mathrm{x}} = \frac{\partial \mathrm{C}_2}{\partial \mathrm{t}} \tag{1}$$

where C_2 is the total concentration of fluorescein (or equivalently fluorescence) in the stroma, D is the average diffusivity in the stroma, and v is the net convection velocity of the fluid in the stroma. The effective diffusivity depends both on the true diffusivity of the solute in stroma and on the binding of the solute to the polymer in the stroma, with an increased binding leading to reduced effective diffusivity. The boundary conditions for Eq. 1 at the interfaces formed with the endothelial and the epithelial layers will be discussed below.

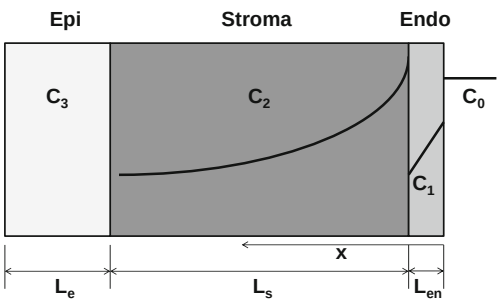

Fig. 5 Schematic representation of the transport of fluorescein from the Anterior Chamber toward the tear side. Abbreviations: C_1 Concentration in endothelium; C_2 Concentration in stroma; C_3 Concentration in epithelium; C_0 Fixed concentration in the anterior chamber; x Depth across cornea. The partition coefficient Φ_{ij} represents the ratio of concentrations in region i and j at equilibrium, e.g., Φ_{12} is the ratio of concentration in endothelium and stroma at equilibrium. Fluorescein partitions from a/c to endothelium, and then it diffuses across endothelium into stroma. The transient diffusion in stroma creates a boundary layer, which reaches the epithelium-stroma boundary in about 300 min. Fluorescein then partitions into epithelium and continues to diffuse toward the tear side.

Transport in the Endothelium

Transport across the endothelium can occur through two routes: paracellular (i.e., transport through tight junctions) and transcellular (i.e., transport across the cells). Due to the relatively hydrophilic nature and the small molecular weight of fluorescein (376 Da), its permeation through the paracellular route can be expected. The transcellular flux, on the other hand, requires the molecules to traverse the lipid bilayers of the endothelium. The cross-sectional area for paracellular transport being much smaller compared to that for the transcellular transport, the flux through the latter route could be the prominent mechanism. When measuring the permeability of the endothelium using Ussing chambers, it is not feasible to determine the dominant mechanism. However, the accumulation of fluorescein in the endothelium, as evident in the profiles in Fig. 2 shows that the solute must cross the lipid bilayers to accumulate inside the cytoplasm. In addition, as mentioned earlier, the ratio of the fluorescence in the endothelium and that in the stroma at the interface with the endothelium is relatively constant (Fig. 4), suggesting that the two concentrations are in equilibrium due to transport through the lipid bilayers of the cells. Based on these considerations, we propose the following mass balance across the endothelium to define fluorescein transport:

$$V_E\frac{\partial \mathrm{C}_1}{\partial \mathrm{t}} = \mathrm{kA}\left(\mathrm{Co} - \frac{\mathrm{C}_1}{\emptyset_{10}}\right) - \mathrm{kA}\left(\frac{\mathrm{C}_1}{\emptyset_{12}} - \mathrm{C}_2\right) \tag{2}$$

where C_1 is the concentration in the endothelium, C_o is the concentration in the Ringers bathing the endothelial surface, ϕ_{10} is the partition coefficient of fluorescein between

the cytoplasm of the endothelium and the aqueous humor, ϕ_{12} is the partition coefficient between the cytoplasm in the endothelium and the stroma, and k is the permeability of the endothelial lipophilic membranes. In the equation above, the first term on the right-hand side accounts for the net transport from the a/c to the endothelium, while the second term defines the net transport from the endothelium to the stroma. The surface area A is the transcellular area available for transport, and V_E is the volume of the endothelium.

The endothelium is coupled to the stroma through the following boundary condition:

$$-\mathrm{D}\frac{\partial \mathrm{C}_2}{\partial \mathrm{x}} = \mathrm{kA}\left(\frac{\mathrm{C}_1}{\emptyset_{12}} - \mathrm{C}_2\right) \tag{3}$$

The diffusion resistance in the stroma (L_s/D) is much larger than that in the endothelium (1/k) because of the larger thickness of the stroma in comparison to that of the endothelium (this assumption is verified later after comparing the estimated parameter values). Accordingly, the above boundary condition can be simplified to:

$$\mathrm{C}_2 = \frac{\mathrm{C}_1}{\emptyset_{12}} \tag{4}$$

This simplification implies that the stromal concentration at the interface is in equilibrium with that in the endothelium, which is clearly supported by the data in Fig. 4. This simplified boundary condition can now be applied in the governing equation for the endothelium (Eq. 2) to yield the following simplified mass balance for the endothelium:

$$V_E\frac{\partial \mathrm{C}_1}{\partial \mathrm{t}} = \mathrm{kA}\left(\mathrm{Co} - \frac{\mathrm{C}_1}{\emptyset_{10}}\right) \tag{5}$$

The above equation can be solved by using C_1=0 as the initial condition to get the following expression for the endothelial concentration:

$$\mathrm{C}_1 = \emptyset_{10}\mathrm{Co}\left(1 - e^{\frac{-kAt}{V_E\emptyset_{10}}}\right) = \emptyset_{10}\mathrm{Co}\left(1 - \mathrm{e}^{-\mathrm{k}_1\mathrm{t}}\right) \tag{6}$$

where:

$$k_1 \equiv \frac{\mathrm{kA}}{V_E\emptyset_{10}} \tag{7}$$

Using Eq. 7 in Eq. 4, we get the following boundary condition for transport across the stroma at the stroma-endothelium interface:

$$C_2 = \emptyset_{21}\emptyset_{10}Co\left(1 - e^{-k_1t}\right) = \emptyset Co\left(1 - e^{-k_1t}\right) \tag{8}$$

where $\emptyset_{21}(= 1/\emptyset_{12})$ is the partition coefficient of the drug between the stroma and the cytoplasm in the endothelium. It should be noted that $\emptyset = \emptyset_{21} \times \emptyset_{10}$ is the effective partition coefficient of the drug between the stroma and the Ringers solution bathing the endothelial surface.

Transport in the Epithelium

Based on the transport in the endothelium, the mechanism for the epithelium is likely to be transcellular as well. However, due to the multiple layers, the epithelium is expected to offer significantly larger resistance to transport, and hence we assume that for short periods of time (< 200 min), the flux from the stroma to the epithelium is essentially zero. Thus:

$$-\mathrm{D}\frac{\partial \mathrm{C}_2}{\partial \mathrm{x}} + \mathrm{vC}_2 = 0 \tag{9}$$

This simplified model cannot predict the concentrations in the epithelium. The validity of the above assumption can be evaluated by noting that the epithelial concentrations are significantly less than the concentrations in the endothelium, and additionally, the slope of the fluorescence profiles is negligible at the epithelium-stroma interface.

The governing equation for the transport in the stroma (Eq. 1), along with the boundary conditions (Eqs. 8 and 9) can be solved numerically by finite difference to obtain the concentration profiles as a function of time in the stroma and the concentration transients in the endothelium. It is to be noted that the model presented above has no non-linear terms. Therefore, the response is linearly proportional to the solute concentration in the a/c. Furthermore, if the fluorescence is linearly proportional to the concentration with the same constant of proportionality in each layer, the concentration can simply be expressed in fluorescence units. Based on these assumptions, we interchangeably use fluorescence for fluorescein concentration below.

Parameter Estimation

The procedure for parameter estimation is similar to the strategy that we employed for the data of Rhodamine B previously (4). Briefly, we first recall that the fluorescence at any location x is obtained by convolution of the predicted fluorescein profile and the Instrument Response Function (IRF). Thus,

$$\mathrm{C}_{\mathrm{Model}}(\mathrm{x}') = \int_0^\infty \mathrm{C}(\mathrm{x})\ \mathrm{IRF}(\mathrm{x} - \mathrm{x}')\mathrm{dx} \tag{10}$$

where

$$\mathrm{IRF}(\mathrm{x} - \mathrm{x}') = \frac{\mathrm{e}^{-\left(\frac{(\mathrm{x}-\mathrm{x}')}{\sqrt{2\sigma^2}}\right)^2}}{\sqrt{2\pi\sigma^2}} \tag{11}$$

where (2.36σ) represents the full width of the Gaussian profile of the IRF, which is taken as 20 μm as before. The unknown

model parameters (D, v, ϕ, k_1) are next obtained by matching the model prediction to the experimental data by minimizing the following objective function E, which is the sum of the squares of the difference between the model and the experimental results.

$$E = \sum_{i=1}^{N} \left[\left(C_{Model} - C_{Exp} \right)^2 \right]_i \quad (12)$$

where C_{exp} and C_{Model} are the measured and predicted concentrations at the given position and time, and N represents the total number of data points. The four unknown parameters can be obtained by fitting all the data in the stroma and the endothelium, or alternatively, the parameter k_1 can first be determined by fitting the endothelial data, and the remaining three parameters can be obtained by fitting the stromal data. We adopt the second approach as the endothelial data are highly sensitive to the parameter k_1, and thus, more reliable values of k_1 can be obtained by fitting the endothelial concentration or, equivalently, the stroma concentration at the stroma-endothelium interface. The remaining three parameters were obtained by minimizing the sum of the squares (Eq. 12) in the stroma. The values of the fitted parameters are presented in Table I, and the best fit fluorescence profiles are compared with the experimental data in Fig. 6. It is noted that a model in which the endothelium is treated as a membrane with constant permeability, which is a suitable model for paracellular transport, cannot fit the experimental data (results not shown). This further supports the hypothesis that transport of fluorescein through the endothelium is dominated by transcellular transport.

Sensitivity Analysis of the Parameters

To further address the robustness of the model, it is important to show that the parameters in Table I are unique. We adopted various approaches to test the reliability of the three parameters (D, v, and ϕ), including construction of contour plots, and calculation of correlation coefficients and sensitivity indices.

Table I The Optimal Values of the Model Parameters Obtained by Minimizing the Total Error Between the Model Prediction and Experimental Data. Ø, D, and v are Obtained by Fitting the Time- and Position-Dependent Stroma Data, and the Parameter k_1 is Obtained by Fitting the Time-Dependent Data from the Stroma-Endothelium Boundary. Sensitivity Analysis of the Transport Model. Values of the Sensitivity Index Larger than 5 Indicate that Error Between the Experimental Data and the Model Fit Increased by Less than 5% for a 10% Change in the Model Parameter, which Implies a Robust Fit and a Reliable Value of the Fitted Parameter

Parameter	Estimated Value	Units	Sensitivity Index
Φ	1.79	–	132.8
k_1	0.12	hr^{-1}	94.0
D	7.76×10^{-12}	m^2/s	17.8
v	1.38×10^{-8}	m/s	4.3

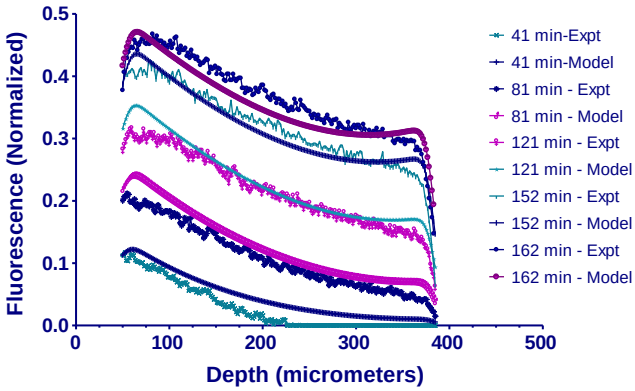

Fig. 6 Comparison of the model predictions and the experimental profiles of the fluorescein concentration in the stroma for short durations ($t < 3$ h) using the best-fit values of the parameters D, v, and φ. Here $x = 384$ μm represents the epithelium-stroma interface while $x = 50$ μm represents the stroma-endothelium interface. The time at which the profiles are compared is indicated on each curve.

The contour plots were constructed by choosing two parameters, varying them within ±50% of their estimated values, and plotting the contours along which the error E, as defined in Eq. 12, is constant. The shapes of the contour plots reflect the correlation between the two parameters that are varied for the plot. For instance, if the contour plots around the minimum are concentric and culminate in a point or a small line segment, we are assured that the parameters are not correlated around the estimated values. However, if the contours are elliptic, culminating in a line, it implies that the parameters are correlated, i.e., changes in one parameter can be compensated by changes in the other parameter, and thus, accurate determination of the parameters is not possible. If, on the other hand, the contours are vertical (or horizontal lines), the error is independent of the parameter on the x axis (or y axis for horizontal contours). The plots in Fig. 7a and b show that the contours for ϕ-D and ϕ-v pairs converge onto a single point, which mean that these parameters are well identified. The contour plots for the D-v pair (Fig. 7c) show that, close to the location of the minimum error, there are multiple contours that have similar error values, which implies the existence of multiple local minima. In this case, the parameter estimation may depend on the initial guesses of the parameters. However, the three minima are relatively close to each other, and thus, the best-fit values in Table I are reliable.

The qualitative information in the contour plots can be quantified by computing the correlation coefficients between various pairs of parameters. Such coefficients for each pair of parameters are presented in Table II. They lie between −0.9 and 0.9, indicating that the parameters are uncorrelated.

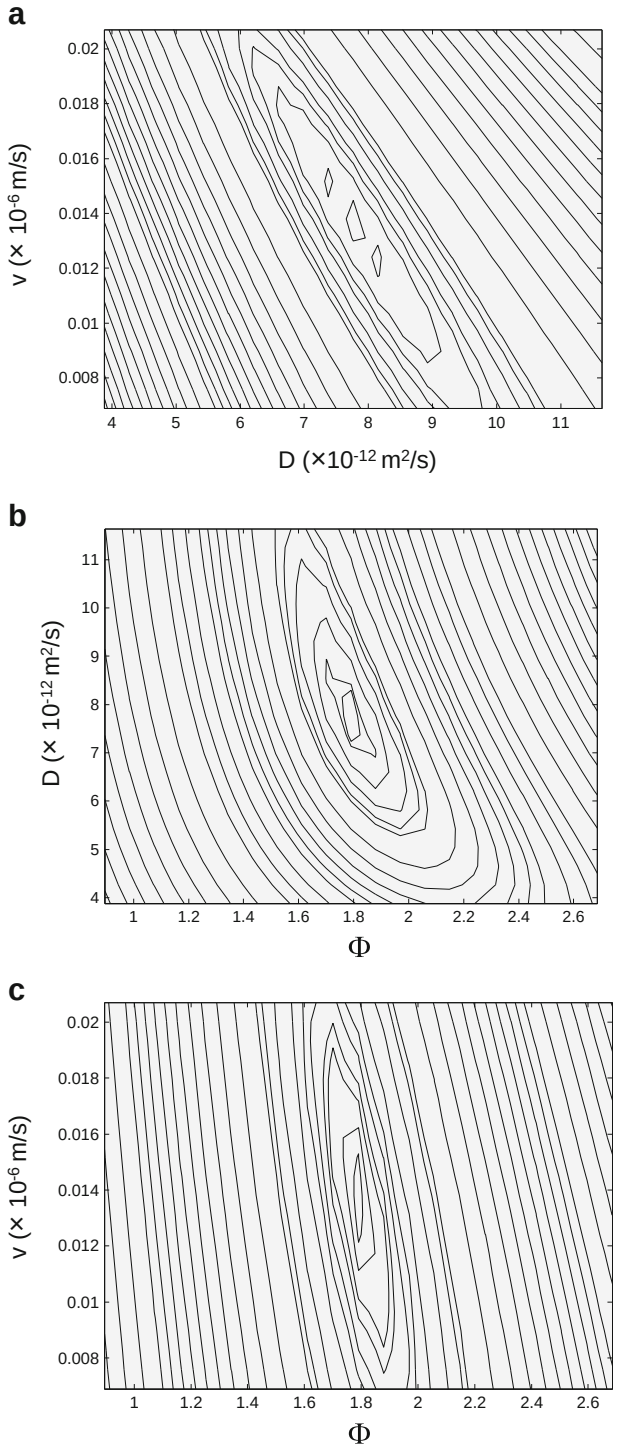

Fig. 7 Contour plots of error, i.e., square of the difference between the model predictions and experimental values for fluorescence in cornea. The error is constant along any contour. The parameters on the x and the y axes are varied in a range of ±50% around the optimal values, while keeping all other variables fixed at the optimal values. The contours for (**a**) (D, φ) and (**b**) (v, φ) show a single minimum, and contours converge, proving that the fitting is robust. Contours for (**c**) (D, v) show three local maxima, which implies that the optimized values of the fitted parameters depend on the initial choice. All three maxima are, however, relatively within a narrow region, which implies that the variations in the fitted values due to initial choice are small.

To further examine the sensitivity of each model parameter, we determined sensitivity index, which is a measure of the relative increase in error E, as defined in Eq. 12, for changes in that parameter. A large value of the index value implies that small changes in the parameter lead to relatively large changes in the error, and thus, the parameter value is robust. Since all parameters except one are fixed in this analysis, the error can be expanded as a Taylor series around the point of minimum error:

$$E = E_{\min} + \frac{1}{2}\frac{d^2E}{du^2}\bigg|_{u_{\min}} (u - u_{\min})^2 \tag{13}$$

where E_{min} is the minimum error or the error corresponding to the predicted parameter, u is the specific parameter (any one of the four model parameters), and u_{min} is the value of u at which the error is the minimum or the estimated value of u. It is noted that the linear term is absent from the above expansion because the first derivative, dE/du is zero at the minimum. As discussed previously (4), the sensitivity index α is defined by the following equation:

$$\alpha = \frac{\left[\frac{E-E_{\min}}{E_{\min}}\right]}{\left[\frac{u-u_{\min}}{u_{\min}}\right]^2} \equiv \frac{u_{\min}{}^2}{2E_{\min}}\frac{d^2E}{du^2}\bigg|_{u_{\min}} \tag{14}$$

The second derivative of E was obtained by computing E around u_{min} in the range $-0.05\ E_{min} < (E - E_{min}) < 0.05\ E_{min}$ and then fitting the data to a quadratic polynomial (without the linear term). Equation 14 was then used to calculate the value of α for all the parameters, and the results are presented in Table I. All sensitivity indices are about 5 or larger, which again implies that the model is sensitive to each of the parameters.

Hydraulic Permeability of the Cornea

The convection through the cornea is generated because the continuous flow of fluid into the a/c creates a pressure difference across the cornea. The velocity of the fluid obtained by the approach described above can be utilized to compute the hydraulic permeability of the cornea. According to Darcy's

Table II Coefficient of Correlation Between all the Model Parameters Obtained by Fixing All Parameters Except the Two Chosen Parameters. Correlation Coefficient is Calculated for the Limiting Contours Encompassing the Minima. Coefficient of Correlation Should Lie Between −0.9 and 0.9 for Variables to be Uncorrelated

Parameter	Φ	D	v
Φ	I	−0.58	0.09
D		I	−0.33
v			I

law, the specific hydraulic conductivity of a porous medium, K, can be obtained by the following expression (16):

$$K = -\frac{\mu U l}{\delta P} \tag{15}$$

where μ is the fluid viscosity, U is the fluid velocity in the medium, l is the length or depth of the medium, and δP is the pressure gradient across the porous media. We measured a pressure gradient of 20 cm of water on the endothelial side as the epithelium side was exposed to atmosphere (pressure loss due to flow of viscous fluid through the tubes pipe is calculated to be negligible). In addition, using velocity obtained by fit from the model (Table I), the viscosity of 1 cP for water, and the thickness of the stroma at 340 μm (Fig. 3), we obtain the specific hydraulic conductivity of the medium to be 2.4×10^{-14} cm^2.

Permeability of the Epithelium

The permeability of the epithelium is likely to be much smaller than the permeability of the endothelium, and thus, it was neglected in the analysis presented above. Due to the small permeability, the epithelial concentration is negligible (undetectable) during the first 150 min, which is the duration utilized for modeling the stromal profiles. At longer times, both the stroma and the epithelium swell, complicating the transport processes. As noted earlier, based on the transport across the endothelium, it can be expected that the dominant transport mechanism is transcellular transport through the lipid bilayers. Since the detailed fluid transport during swelling has not been measured, it is it is not feasible to develop a detailed model for corneal transport. Accordingly, a simple model is developed to estimate the permeability of the epithelium.

We model epithelium as a well-mixed compartment of volume V_{Epi} that is in contact with the stroma on one side and tears on the other side. Furthermore, the concentration on the tear side can be assumed to be zero due to continuous clearance. The concentration in the epithelium can thus be described by the following mass balance:

$$V_{Epi}\frac{dC_e}{dt} = A\left(k_{se}\left(\frac{C_s}{\phi_{se}} - C_e\right) - k_{et}C_e\right) \tag{16}$$

where C_e is the average concentration in the epithelium (spatial average of C_3), A is the cross-sectional area of the cornea, k_{se} is the permeability of the epithelium at its stromal interface, C_s is the concentration in the stroma at the stroma-epithelium interface, ϕ_{se} is the partition coefficient of fluorescein between the stroma and the epithelium, and k_{et} is the permeability of the epithelium. The epithelial concentration is far from equilibrium, as evident from the fact that the concentration in the epithelium is much less than that in the endothelium. The above equation can then be simplified in the short time regime to the following form:

$$\frac{dC_e}{dt} = \frac{A}{V_e}k_{se}\frac{C_s}{\phi_{se}} \tag{17}$$

The above equation can be integrated to get:

$$C_e = \frac{k_{se}}{h_{Epi}\,\phi_{se}}\int C_s(t)dt \tag{18}$$

where h_{Epi} is the epithelial thickness assumed to have an average value of 40 μm (Fig. 3). To get the permeability, k_{se}, ϕ_{se} is assumed to have a similar value as the partition coefficient for the stroma-endothelium interface due to the very similar structural properties of the epithelium and the endothelium. A rough estimate of the partition coefficient of the stroma-endothelium interface, ϕ_{21}, is obtained as 2.05 by plotting the stromal concentration at this interface as a function of the endothelium concentration. The experimentally obtained concentration profiles for the epithelium concentration as a function of time are fitted to Eq. 17 (Fig. 8) to obtain the permeability of the epithelium-stroma interface (equal to 0.92×10^{-9} m/s).

Comparison of Fitted Values to Previously Reported Values

The sensitivity analysis suggests that parameters are well identified, and the model clearly explains the important characteristics of the experimental data. However, to further test the validity of the model, it is useful to compare the fitted model parameters with prior values reported in the literature.

The effective diffusivity, D, in the stroma has been reported to be 1.21×10^{-10} m^2/s (17), which is an order higher than the estimated value in this study (Table I). The discrepancy could perhaps be caused by significant

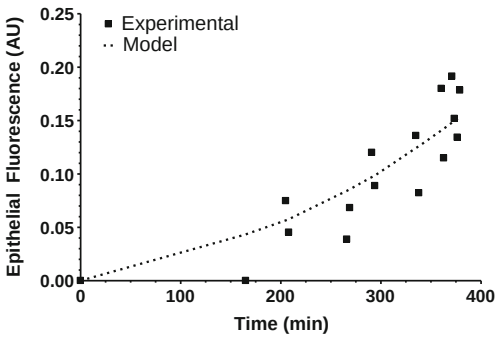

Fig. 8 Comparison of the model prediction and experimental data for the epithelial concentration. Epithelial permeability is obtained by minimizing the error between the experimentally measured concentration profiles and the model prediction.

differences in the experimental design or due to differences in assumptions regarding the physical situation. In addition, Φ, the partition coefficient between the stroma and the aqueous humor, has been measured to be 1.33 (17), 1.5 (18), and 1.90 (9), which is in good agreement with our model prediction of 1.79 (Table I). Johnson *et al.* have used quick freeze/deep-etch method to morphometrically predict specific hydraulic conductivity of corneal stroma to be between 0.46×10^{-14} cm^2 and 0.3×10^{-14} cm^2 (19). Also, hydraulic conductivity measured through experimental methods available in the literature ranges between 0.5×10^{-14} cm^2 and 2×10^{-14} cm^2 (19). We calculate hydraulic conductivity to be 2.4×10^{-14} cm^2, which is in close agreement with both the morphometric and experimental values reported so far. The low epithelial permeability (8) justifies our assumption of zero flux into the layer for short time scales. In addition, our estimate of epithelial permeability of 0.92×10^{-9} m/s in rabbits is within the range of values reported by Araie and Maurice (8) as 4.3×10^{-9} m/s and Hughes and Maurice (20) as 0.5×10^{-9} m/s. Based on the estimated value of the parameter k_1, using an average value of the endothelial thickness of 13 μm (obtained from experimental profiles), $\emptyset_{10} = \emptyset/\emptyset_{21} = 0.87$, and assuming the area of the paracellular route as negligible in comparison to the transcellular route, we predict the endothelial permeability to be 0.37×10^{-9} m/s (Eq. 7). This value is expectedly of the same order as the estimated value for epithelial permeability due to the structural similarities of both layers, but it is different from previously reported values in the literature (9). Nevertheless, the low endothelial permeability justifies our theory of transcellular flux as the dominant mechanism.

CONCLUSION

A mechanistic depth-resolved pharmacokinetic model has been developed for the transient transport of fluorescein in the rabbit cornea. The experimental data accompanied by the model suggests that apart from traversing through the paracellular route, fluorescein is transported across by the transcellular route, which leads to a persistent increase in concentration of the dye in the endothelium. This study also shows that the transport of fluorescein through the excised cornea occurs through a combination of diffusion and convection. The convection, however, might be absent under *in vivo* conditions. The parameters used in fitting the model to the experimental results are independent and accurately characterize the transport of fluorescein. The fitted values are reliable with low uncertainty values and are sensitive to the model. This study improves the fundamental understanding of transport of hydrophilic molecules through cornea and presents a framework that could be used to model transport of hydrophilic drugs or other solutes in a human cornea.

ACKNOWLEDGMENTS AND DISCLOSURES

This study was supported by NIH grant R21-EY019119 (SPS).

REFERENCES

1. Gaudana R, Ananthula HK, Parenky A, Mitra AK. Ocular drug delivery. AAPS J. 2010;12:348–60.
2. Ghate D, Edelhauser HF. Ocular drug delivery. Expert Opin Drug Deliv. 2006;3:275–87.
3. Klyce SD. Electrical profiles in the corneal epithelium. J Physiol. 1972;226:407–29.
4. Gupta C, Chauhan A, Mutharasan R, Srinivas SP. Measurement and modeling of diffusion kinetics of a lipophilic molecule across rabbit cornea. Pharm Res. 2010;27:699–711.
5. Srinivas SP. Dynamic regulation of barrier integrity of the corneal endothelium. Optom Vis Sci. 2010;87:E239–54.
6. Srinivas SP. Cell signaling in regulation of the barrier integrity of the corneal endothelium. Exp Eye Res. 2012;95:8–15.
7. Araie M. Kinetics of intraocular penetration of topical fluorescein: analysis by new method. Jpn J Ophthalmol. 1983;27:421–33.
8. Araie M, Maurice D. The rate of diffusion of fluorophores through the corneal epithelium and stroma. Exp Eye Res. 1987;44:73–87.
9. Araie M, Maurice DM. A reevaluation of corneal endothelial permeability to fluorescein. Exp Eye Res. 1985;41:383–90.
10. Cheeks L, Kaswan RL, Green K. Influence of vehicle and anterior chamber protein concentration on cyclosporine penetration through the isolated rabbit cornea. Curr Eye Res. 1992;11:641–9.
11. Chien DS, Tang-Liu DD, Woodward DF. Ocular penetration and bioconversion of prostaglandin F2alpha prodrugs in rabbit cornea and conjunctiva. J Pharm Sci. 1997;86:1180–6.
12. Hamalainen KM, Kananen K, Auriola S, Kontturi K, Urtti A. Characterization of paracellular and aqueous penetration routes in cornea, conjunctiva, and sclera. Invest Ophthalmol Vis Sci. 1997;38:627–34.
13. Kawazu K, Midori Y, Shiono H, Ota A. Characterization of the carrier-mediated transport of levofloxacin, a fluoroquinolone antimicrobial agent, in rabbit cornea. J Pharm Pharmacol. 1999;51:797–801.
14. Maurice DM, Srinivas SP. Fluorometric measurement of light absorption by the rabbit cornea. Exp Eye Res. 1994;58:409–13.
15. Srinivas SP, Maurice DM. A microfluorometer for measuring diffusion of fluorophores across the cornea. IEEE Trans Biomed Eng. 1992;39:1283–91.
16. Levick JR. Flow through interstitium and other fibrous matrices. Q J Exp Physiol. 1987;72:409–37.
17. Nagataki S, Brubaker RF, Grotte DA. The diffusion of fluorescein in the stroma of rabbit cornea. Exp Eye Res. 1983;36:765–71.
18. Shiraya K, Nagataki S. Movement of fluorescein monoglucuronide in the rabbit cornea. Diffusion in the stroma and endothelial permeability. Invest Ophthalmol Vis Sci. 1986;27:24–8.
19. Overby D, Ruberti J, Gong H, Freddo TF, Johnson M. Specific hydraulic conductivity of corneal stroma as seen by quick-freeze/deep-etch. J Biomech Eng. 2001;123:154–61.
20. Hughes L, Maurice DM. A fresh look at iontophoresis. Arch Ophthalmol. 1984;102:1825–9.